Neurobiology of Aging 165 (2026) 1–7

Contents lists available at ScienceDirect

Neurobiology of Aging

journal homepage: www.elsevier.com/locate/neuaging.org

# An exploratory analysis of plasma biomarkers associated with cerebral amyloid angiopathy

Ersin Ersözlü [a,b,c,*], François Meyer [a,b,d], Lukas Preis [a,b,c], Orkan Arslan [a], Daria Gref [a,b,c], Louise Droste [a,b,c], Julian Hellmann-Regen [a,b,c], for the Alzheimer's Disease Neuroimaging Initiative[1]

[a] Charité – Universitätsmedizin Berlin, Corporate Member of Freie Universität Berlin and Humboldt Universität zu Berlin, Department of Psychiatry and Neurosciences, Hindenburgdamm 30, Berlin 12203, Germany
[b] Charité – Universitätsmedizin Berlin, Corporate Member of Freie Universität Berlin and Humboldt Universität zu Berlin, ECRC Experimental and Clinical Research Center, Lindenberger Weg 80, Berlin 13125, Germany
[c] German Center for Neurodegenerative Diseases (DZNE) within the Helmholtz Association, Berlin, Germany
[d] Neurocognitive Disorders Research Group, GIGA Clinical Neurosciences, University of Liège, Liège, Belgium

ARTICLE INFO

*Keywords:*
Cerebral amyloid angiopathy
Alzheimer's disease
Plasma biomarkers
Cerebral microbleeds
Neuropathology

ABSTRACT

Cerebral amyloid angiopathy (CAA) remains diagnostically challenging, particularly in asymptomatic individuals. While CAA often co-exists with Alzheimer's disease (AD), it may even have a direct impact on AD pathophysiology and the cognitive decline within the clinical course of AD. While fluid biomarkers are well established for AD pathology, reliable markers to characterize CAA are lacking. We analyzed two subsets of participants from the Alzheimer's Disease Neuroimaging Initiative with available plasma biomarker measurements from a 145-analyte multiplex immunoassay panel: one with T2*-weighted gradient-echo magnetic resonance imaging (MRI) data (n = 21) and another with postmortem neuropathological data (n = 24). We defined CAA as ≥ 2 lobar microbleeds on MRI or moderate-to-severe neocortical amyloid angiopathy on neuropathological examination. Plasma analytes were assessed twice per participant, one year apart, with the earlier sample obtained up to 6.6 years prior to either the first MRI or neuropathological examinations. In both cohorts, various markers related to inflammation, lipid metabolism, and cell adhesion were associated with CAA proxy measures. Specifically, both increased (Fas ligand receptor, Receptor for Advanced Glycosylation End-Products, Osteopontin, and Vascular Cell Adhesion Molecule-1) and decreased (Vitronectin, Endothelial Growth Factor) biomarker levels were associated with lobar microbleeds, while increased apolipoproteins (ApoAII, ApoCI, ApoCIII, ApoE, and clusterin) and decreased AXL were associated with CAA severity in neuropathology. Ratios between inversely associated markers enhanced correlation strength and differed between CAA and non-CAA. Given the small sample sizes in our exploratory analyses, larger studies are required to evaluate the discriminatory potential and clinical translatability of the identified biomarkers for CAA.

## 1. Background

Cerebral amyloid angiopathy (CAA) is a cerebrovascular disorder caused by the build-up of β-amyloid (Aβ) in the walls of leptomeningeal and cortical blood vessels. CAA affects 25% of the general elderly population (Jäkel et al., 2022) and can clinically manifest with intracerebral hemorrhage, temporary disturbances in cortical functions (such as motor, somatosensory, visual, or language functions), and progressive cognitive decline (Cozza et al., 2023). CAA and Alzheimer's disease (AD) share key pathological characteristics; however, in AD, Aβ plaques primarily accumulate in the brain parenchyma adjacent to neurons, whereas in CAA, they deposit in cerebral blood vessels (Attems et al., 2005; Weller et al., 2008). Notably, CAA co-occurs with AD in approximately 50% of cases (Jäkel et al., 2022).

* Correspondence to: Klinik für Psychiatrie und Psychotherapie, Gedächtnissprechstunde, Hindenburgdamm 30, Berlin 12203, Germany.
*E-mail address:* ersin.ersoezlue@charite.de (E. Ersözlü).

[1] Data used in preparation of this article were obtained from the Alzheimer's Disease Neuroimaging Initiative (ADNI) database (adni.loni.usc.edu). As such, the investigators within the ADNI contributed to the design and implementation of ADNI and/or provided data but did not participate in analysis or writing of this report. A complete listing of ADNI investigators can be found at: http://adni.loni.usc.edu/wp-content/uploads/how_to_apply/ADNI_Acknowledgement_List.pdf.

https://doi.org/10.1016/j.neurobiolaging.2026.04.004
Received 8 December 2025; Received in revised form 14 April 2026; Accepted 15 April 2026
Available online 21 April 2026

Previously, diagnosing CAA relied on postmortem examination of brain tissue. The introduction of the Boston Criteria enabled the in vivo diagnosis of CAA, defining "possible" or "probable" CAA based primarily on clinical and magnetic resonance imaging (MRI) findings, such as lobar microbleeds (MBs) (Knudsen et al., 2001). The Boston Criteria v2.0 has notably expanded the criteria to include clinical features and non-hemorrhagic findings (Charidimou et al., 2022). However, when applied to asymptomatic patients or those with cognitive impairment, the v.2.0 criteria revealed a 28.6% sensitivity and 65.3% specificity for "probable CAA" alone (Switzer et al., 2024). This can be considered rather low, compared to diagnostic performances in the field of AD, where fluid biomarkers in cerebrospinal fluid (CSF) and plasma have evolved into reliable diagnostic tests (Graff-Radford et al., 2021). Only a limited number of studies have addressed the unmet need for accurate diagnostic approaches to CAA. These studies found that CAA may be associated with lower CSF levels of Aβ40 and Aβ42, while CAA-related inflammation has been linked to microglial and T cell activation, as well as increased CSF tau concentrations (Hampel et al., 2023; Theodorou et al., 2021).

Given the heterogeneous clinical manifestations and the limited diagnostic accuracy of current strategies, we conducted an exploratory analysis to identify candidate plasma markers of CAA using MRI and neuropathological indicators.

## 2. Methods

### 2.1. Participants

Data used in the preparation of this article were obtained from the Alzheimer's Disease Neuroimaging Initiative (ADNI) database (adni.loni.usc.edu). Participants included in our analyses were recruited for the prospective Alzheimer's Disease Neuroimaging Initiative (ADNI)-1 convenience cohort (National Clinical Trial (NCT): 00106899), while MRI data were acquired during follow-up visits within ADNI-GO, ADNI-2, and ADNI-3 convenience cohorts (NCT00106899, NCT01231971, and NCT02854033). According to the ADNI protocol, all procedures performed in the study involving human participants were conducted in accordance with the ethical standards of the institutional and/or national research committees. Experiments were undertaken with the understanding and written consent of each participant. All local institutional review boards and ethical committees approved the study protocol.

A summary of inclusion and exclusion criteria and detailed characteristics of the included study sample are provided in the supplementary material. In short, we included participants with available plasma biomarkers and either visual assessments of MBs in T2*-GRE MRI (cohort-MRI, n = 21) or postmortem neuropathological assessments (cohort-NP, n = 24) (Supplementary Figure 1).

### 2.2. Study design

For the primary analysis, we selected a time point (T0) when all multiplex panel measurements (MPM) were accessible. Using a longitudinal approach, we also investigated the association of a second MPM after 1 year (T1) with radiologic assessments of lobar MBs (Fig. 1A) and neuropathological findings indicative of CAA (Fig. 1B), respectively.

### 2.3. Fluid biomarkers

For the plasma measurements, we included all available analytes (n = 145) in the multiplex immunoassay panel, consisting of proteins related to cancer, cardiovascular disease, metabolic disorders, inflammation, and AD— see Supplementary Table 1. Notably, plasma analytes were measured at time points T0 and T1, separated by a 1-year interval. Summarized descriptions of measurements of plasma and CSF markers are presented in the supplementary material. The plasma samples were analyzed by using the Luminex xMAP (Multi-Analyte Profiling) technology, while the CSF samples were analyzed using the electrochemiluminescence immunoassay (ECLIA) Elecsys on a fully automated Elecsys cobas e instrument (Roche Diagnostics GmbH, Penzberg, Germany). The cut-off value of 0.1 was defined for phosphorylated-tau181/Aβ1–42, as reported elsewhere (Shaw et al., 2009).

### 2.4. Cranial MRI acquisition and analysis

The imaging protocol includes multicentric 3 T MRI examinations, including GE, Siemens, and Philips MRI Systems, among others, including T2*-GRE sequences (repetition time (TR) 650 ms, echo time (TE) 20 ms, flip angle (FA) 20 °) and T1-MPRAGE (TR 2300 ms, TE 2.95 ms, FA 9 °) sequences. T2* imaging enables in vivo detection of microhemorrhage-derived hemosiderin deposits as a hypointense signal.

Detailed descriptions of MB detection and atlas assignment methods have been reported in the ADNI Methods document, available at http://adni.loni.usc.edu/. A summary of image acquisition parameters, as well

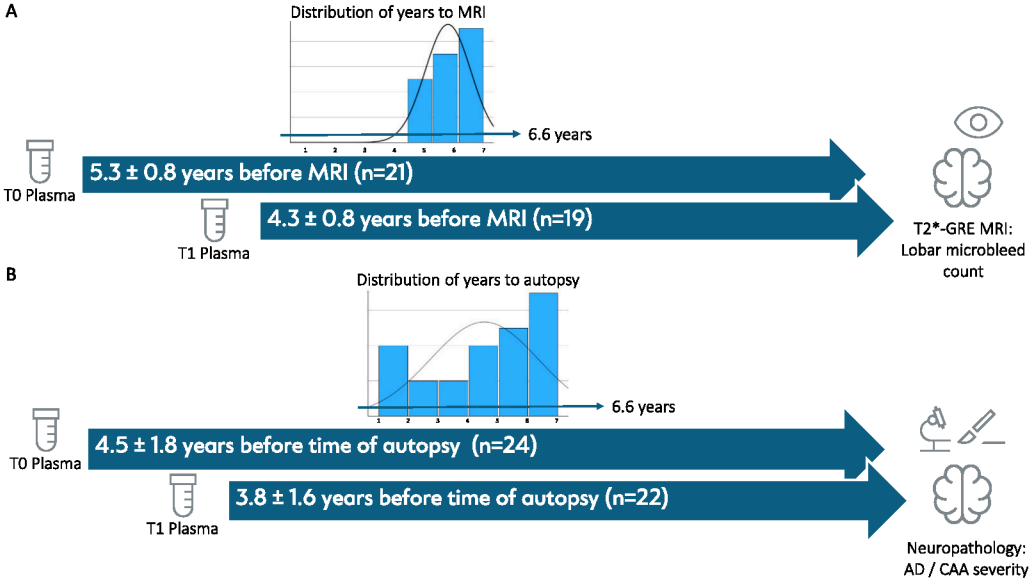


**Fig. 1.** Graphical summary of the study design. Abbreviations: AD, Alzheimer's disease; CAA, cerebral amyloid angiopathy.

as quality and radiological visual assessments, is also provided in the supplementary material. Notably, participants with two or more lobar MBs have been classified as having CAA (Charidimou et al., 2022).

### 2.5. Neuropathological assessment

Pathological lesions in the brain were assessed at autopsy using established neuropathologic diagnostic criteria, as detailed in the ADNI documents at http://adni.loni.usc.edu/.

The central neuropathological severity scales for AD (Variable NPADNC) and CAA (Variable NPAMY) have been included. We included a semi-quantitative (None, low, intermediate, high) assessment for AD using the Alzheimer's Disease – NIA-AA Neuropathological Change level (Hyman et al., 2012). Likewise, the semi-quantitative assessment of overall neocortical amyloid angiopathy refers to the global CAA according to the following scale that refers to the global CAA burden: 0 — None: Absent 1 — Mild: Scattered positivity in parenchymal and/or leptomeningeal vessels, possibly in only one brain area 2 — Moderate: Intense positivity in many parenchymal and/or leptomeningeal vessels 3 — Severe: Widespread (more than one brain area) intensive positivity in parenchymal and leptomeningeal vessels.

Importantly, we classified participants with a 'Moderate' or 'Severe' CAA burden as CAA positive, based on previous literature suggesting its clinical importance (Vidoni et al., 2016).

### 2.6. Statistics

All statistical analyses were performed using SPSS Statistics (IBM, version 29). Figures and confidence interval calculations for visualization were generated in Python (v3.11.6) using pandas (v2.1.4), NumPy (v1.26.2), SciPy (v1.11.4), and matplotlib (v3.8.2). The sample size was not determined a priori; all participants with available data were included. Additional descriptions of the statistical methods are presented in the supplementary material.

In summary, group differences in baseline demographic and clinical variables were assessed using the Mann–Whitney *U* test for continuous variables and the chi-square test for categorical variables. Associations between plasma analytes and CAA proxy measures were evaluated using Spearman's rank correlation.

As a sensitivity analysis, CAA status was binarized within the MRI and NP cohorts and group differences in plasma analytes at T0 were examined using univariate analysis of variance (ANOVA) models. Effect sizes were quantified using partial eta squared ($\eta^2$). Unstandardized regression coefficients (B) representing the group contrast (CAA− vs. CAA+, reference group = CAA+) were extracted from the model. To enhance robustness, given the small sample size, nonparametric bootstrap resampling (1000 iterations) was performed, and bias-corrected and accelerated (BCa) 95% confidence intervals were computed for B.

To account for multiple testing across subsequently defined ratios of analytes, false discovery rate (FDR) correction was applied separately within each cohort, within each ratio family (Vitronectin, Endothelial Growth Factor [EGF], and AXL based ratios), and time point, with a significance threshold of $q < 0.05$.

## 3. Results

### 3.1. Group characteristics

The CAA groups in cohort-MRI and cohort-NP did not differ in demographic, genetic, or clinical features, except for clinical diagnosis (Table 1). Additionally, subgroup analyses by CAA status within both cohorts revealed no differences, except that Aβ42 was lower in the CAA+ group in the NP cohort (Supplementary Table 2).

**Table 1**
Group characteristics among cohorts. Means (± standard deviations) are shown for continuous variables, and numbers (percent) are presented for categorical or ordinal variables if not mentioned otherwise.

| | Cohort-MRI (N = 21) | Cohort-NP (N = 24) | p |
|---|---|---|---|
| Age | 72 ± 9 | 77 ± 7 | 0.08* |
| Female | 6 (27%) | 4 (16.7%) | 0.39† |
| Educational years | 16 ± 3 | 16 ± 2 | 0.65* |
| Clinical Diagnosis | | | 0.004† |
| Cognitively normal | 4 (18%) | 0 (0%) | |
| Mild cognitive impairment | 17 (82%) | 18 (75%) | |
| Dementia | 0 (0%) | 6 (25%) | |
| *ApoE ε4* count | | | 0.37† |
| 0 | 13 (59%) | 10 (41.7%) | |
| 1 | 5 (23%) | 10 (41.7%) | |
| 2 | 3 (14%) | 4 (16.7%) | |
| CSF Phosphorylated-tau181/Beta-Amyloid 1–42 Ratio positive status | 7 (41.2%‡) | 13 (72%‡) | 0.06† |
| Time: Plasma to first MRI, years | 5.3 ± 0.8 | NA | - |
| Time: Plasma to time of autopsy, years | NA | 4.5 ± 1.8 | - |
| Lobar cerebral microbleed count, median (Range) | 0 (0−14) | NA | - |
| ≥ 2 lobar cerebral microbleeds | 4 (19%) | NA | - |
| Plasma panel data available at T1 | 19 (90%) | 22 (92%) | - |
| Alzheimer's Disease – NIA-AA Neuropathological Change level | | | - |
| 0 (None) | NA | 1 (4.2%) | |
| 1 (Low) | NA | 6 (25%) | |
| 2 (Intermediate) | NA | 0 (0%) | |
| 3 (High) | NA | 17 (70.8%) | |
| Cerebral Amyloid Angiopathy – Density | | | - |
| 0 (None) | NA | 2 (8.3%) | |
| 1 (Mild) | NA | 14 (58.3%) | |
| 2 (Moderate) | NA | 2 (8.3%) | |
| 3 (Severe) | NA | 6 (25%) | |

* Mann-Whitney *U* test.
†Chi-square Test.
‡ Percentage among the available cases (available in n = 17 and n = 18 for MRI and NP cohorts, respectively)
‡‡ Percentage among the available cases (available in n = 17)
Abbreviations: MRI, magnetic resonance imaging; NP, neuropathology; ApoE, ApolipoproteinE; NA, not applicable.

### 3.2. Linking plasma biomarkers to CAA proxy measures

The correlation analyses revealed several positive and negative associations. At baseline (T0), positive associations with MB count were observed for markers of adhesion (Vascular Cell Adhesion Molecule 1 [VCAM-1]) and immune response/inflammation (Fas ligand receptor [FASLG], Neutrophil Gelatinase-Associated Lipocalin [NGAL], and Kidney Injury Molecule-1 [KIM-1]). At follow-up (T1), MB count was positively associated with markers of vascular function (Angiopoietin-2, Receptor for Advanced Glycosylation End-Products [RAGE]) as well as immune response/inflammation (osteopontin and Kidney Injury Molecule-1 [KIM-1]) (Supplementary Table 3).

With respect to neuropathological CAA severity, baseline (T0) levels of several apolipoproteins (ApoAII, ApoCI, ApoCIII, ApoE, and clusterin), as well as Complement Factor H (ComFH) and transthyretin (TTR), were positively associated. At follow-up (T1), ApoCIII and clusterin, ComFH, C-peptide, leptin, and proinsulin-intact showed positive associations (Supplementary Table 3).

To address inverse relationships among analytes and inter-individual variability in plasma concentrations, we tested several ratios. At baseline (T0), these ratios strengthened correlations in cohort-MRI (VCAM1/Vitronectin, FASLG/Vitronectin, FASLG/EGF, NGAL/Vitronectin, and RAGE/EGF) and in cohort-NP (ApoCIII/AXL, ApoE/AXL, ComFH/AXL, and TTR/AXL) compared to individual analytes. At follow-up (T1), strengthened associations were observed for several ratios, including RAGE/EGF, NGAL/EGF, osteopontin/Vitronectin, and osteopontin/EGF

in cohort-MRI, and ApoCIII/AXL, clusterin/AXL, ComFH/AXL, and leptin/AXL in cohort-NP (Table 2 and Supplementary Figure 2).

### 3.3. Binarized group differences across plasma biomarker

In the ANOVA at baseline (T0), distinct biomarker patterns were observed between the cohort-MRI and cohort-NP groups based on CAA status (Supplementary Table 4). In the cohort-MRI, significantly higher values were observed for inflammation- and adhesion-related ratios within both the Vitronectin and EGF families, specifically with FASLG and RAGE (Table 3 and Fig. 2A). In contrast, within the cohort-NP, associations were confined to the AXL-based ratio family. ApoAII/AXL, ApoCI/AXL, ApoCIII/AXL, ComFH/AXL and ApoE/AXL demonstrated higher values in individuals with moderate-to-severe CAA (Table 3 and Fig. 2B). Bootstrap-derived 95% confidence intervals supported the direction and magnitude of these associations.

## 4. Discussion

By separately examining ante-mortem (MRI-defined) and post-mortem (neuropathology-defined) indicators of CAA, we observed distinct plasma biomarker patterns across cohorts. While these differences may reflect variation in disease stage, comorbidity burden, or biological processes captured by imaging versus histopathology, alternative explanations must be considered. In particular, the small sample size, differences in clinical and cognitive characteristics between cohorts, and temporal heterogeneity between plasma sampling and outcome assessment may substantially influence the observed associations. Notably, the neuropathology cohort included participants with dementia, in contrast to the MRI cohort. In addition, the two approaches capture distinct aspects of CAA: MRI-defined CAA based on lobar microbleeds reflects a hemorrhagic presentation, whereas neuropathological assessment directly quantifies the extent and distribution of vascular amyloid deposition at autopsy. MRI markers, therefore, represent diagnostic proxies rather than direct measures of amyloid burden (Charidimou et al., 2022), while neuropathological studies characterize CAA based on the severity and anatomical distribution of vascular amyloid pathology (Love et al., 2014). Accordingly, the divergent biomarker patterns observed here likely reflect differences in measurement construct, disease stage, and cohort composition rather than biological specificity alone.

Among other markers, higher FASLG/EGF and FASLG/Vitronectin ratios were observed in participants with more than 2 lobar MBs at both time points. FASLG, also known as CD95L, is associated with astrocyte reactivation and cell apoptosis and has been reported in neuroinflammatory and neurodegenerative diseases, as well as ischemic stroke (Bechmann et al., 2000; Choi and Benveniste, 2004). Moreover, FASLG upregulation has been observed in AD in vitro models and contributes to Aβ-mediated neuronal cell death (Su et al., 2003).

Furthermore, positive associations were observed for osteopontin/EGF and osteopontin/Vitronectin with higher MB counts. Osteopontin is an extracellular phosphoprotein implicated in pathological processes in AD, CAA, and vascular dementia (Chai et al., 2021; Grand Moursel et al., 2019). The mechanisms of osteopontin upregulation in

**Table 2**
Correlations of lobar microbleed count and neuropathological cerebral amyloid angiopathy severity score with plasma analytes. Only results with $p < 0.05$ in both time points are presented. Results with FDR-corrected $p < 0.05$ are marked in bold.

| | | Baseline (T0) | | | | | Follow-up (T1) | | | | |
|---|---|---|---|---|---|---|---|---|---|---|---|
| | | | | | 95% Confidence interval | | | | | 95% Confidence interval | |
| | Analyte | rho | p | p-FDR | Lower Bound | Upper Bound | rho | p | p-FDR | Lower Bound | Upper Bound |
| **MRI - Lobar microbleed count** | Ang2/Vitronectin Ratio | 0.236 | 0.304 | 0.33 | -0.231 | 0.614 | **0.616** | **0.005** | **0.018** | **0.211** | **0.841** |
| | FASLG/Vitronectin Ratio | **0.519** | **0.016** | **0.04** | **0.099** | **0.782** | 0.452 | 0.052 | 0.062 | -0.017 | 0.758 |
| | KIM1/Vitronectin Ratio | **0.505** | **0.02** | **0.04** | **0.080** | **0.774** | 0.45 | 0.053 | 0.062 | -0.02 | 0.757 |
| | NGAL/Vitronectin Ratio | **0.612** | **0.003** | **0.02** | **0.231** | **0.83** | 0.405 | 0.085 | 0.09 | -0.074 | 0.733 |
| | RAGE/Vitronectin Ratio | 0.432 | 0.05 | 0.08 | -0.013 | 0.735 | **0.499** | **0.03** | **0.042** | **0.043** | **0.783** |
| | Osteopontin/ Vitronectin Ratio | 0.367 | 0.102 | 0.12 | -0.091 | 0.696 | **0.548** | **0.015** | **0.023** | **0.11** | **0.808** |
| | VCAM1/Vitronectin Ratio | **0.621** | **0.003** | **0.02** | **0.246** | **0.834** | **0.586** | **0.008** | **0.018** | **0.166** | **0.826** |
| | Ang2/EGF Ratio | 0.446 | 0.043 | 0.08 | 0.004 | 0.742 | **0.706** | **0.0007** | **0.01** | **0.357** | **0.882** |
| | FASLG/EGF Ratio | **0.56** | **0.008** | **0.04** | **0.156** | **0.804** | **0.667** | **0.002** | **0.014** | **0.293** | **0.864** |
| | KIM1/EGF Ratio | 0.033 | 0.889 | 0.89 | -0.416 | 0.469 | -0.032 | 0.897 | 0.9 | -0.49 | 0.44 |
| | NGAL/EGF Ratio | **0.512** | **0.018** | **0.04** | **0.089** | **0.778** | **0.58** | **0.009** | **0.018** | **0.157** | **0.823** |
| | RAGE/EGF Ratio | **0.522** | **0.015** | **0.04** | **0.103** | **0.783** | **0.586** | **0.008** | **0.018** | **0.166** | **0.826** |
| | Osteopontin/EGF Ratio | 0.405 | 0.069 | 0.10 | -0.046 | 0.719 | **0.608** | **0.006** | **0.018** | **0.198** | **0.837** |
| | VCAM1/EGF Ratio | 0.373 | 0.096 | 0.12 | -0.084 | 0.7 | **0.548** | **0.015** | **0.023** | **0.11** | **0.808** |
| **Neuropathological CAA severity** | ApoAII/AXL Ratio | **0.514** | **0.01** | **0.02** | **0.127** | **0.765** | **0.537** | **0.01** | **0.02** | **0.136** | **0.787** |
| | ApoCIII/AXL Ratio | **0.675** | **0.0003** | **0.003** | **0.362** | **0.851** | **0.551** | **0.008** | **0.02** | **0.156** | **0.794** |
| | CLU/AXL Ratio | **0.463** | **0.023** | **0.03** | **0.061** | **0.736** | **0.614** | **0.002** | **0.007** | **0.247** | **0.827** |
| | ComFH/AXL Ratio | **0.53** | **0.008** | **0.02** | **0.148** | **0.774** | **0.631** | **0.002** | **0.007** | **0.274** | **0.836** |
| | ApoCI/AXL Ratio | **0.514** | **0.01** | **0.02** | **0.127** | **0.765** | **0.436** | **0.042** | **0.042** | **0.005** | **0.731** |
| | ApoE/AXL Ratio | **0.514** | **0.01** | **0.02** | **0.127** | **0.765** | **0.51** | **0.015** | **0.021** | **0.099** | **0.772** |
| | C-peptide/AXL Ratio | 0.286 | 0.175 | 0.19 | -0.145 | 0.626 | **0.628** | **0.002** | **0.007** | **0.269** | **0.834** |
| | Proinsulin/AXL Ratio | 0.165 | 0.442 | 0.44 | -0.267 | 0.542 | **0.443** | **0.039** | **0.042** | **0.013** | **0.735** |
| | TTR/AXL Ratio | **0.479** | **0.018** | **0.03** | **0.081** | **0.745** | **0.457** | **0.033** | **0.041** | **0.03** | **0.743** |
| | Leptin/AXL Ratio | 0.33 | 0.116 | 0.15 | -0.1 | 0.654 | **0.512** | **0.015** | **0.02** | **0.102** | **0.773** |

Abbreviations: Ang2, Angiopoietin-2; FASLG, Fas Ligand Receptor; KIM1, Kidney Injury Molecule-1; NGAL, Neutrophil Gelatinase-Associated Lipocalin; RAGE, Receptor for advanced glycosylation end-products; VCAM1, Vascular Cell Adhesion Molecule-1; EGF, Epidermal Growth Factor; Apo, Apolipoprotein; CLU, Clusterin; ComFH, Complement Factor H; TTR, Transthyretin; FDR, false discovery rate.

**Table 3**
Group differences in plasma analytes according to MRI-based and neuropathological diagnosis of cerebral amyloid angiopathy at baseline (T0). Results with false discovery rate (FDR) corrected $p < 0.05$ are shown.

| Cohort | Ratio | B | p | p-FDR | Lower B (95% CI) | Upper B (95% CI) | Partial $\eta^2$ |
|---|---|---|---|---|---|---|---|
| MRI | FASLG/Vitronectin Ratio | -0.094 | 0.004 | 0.013 | -0.154 | -0.035 | 0.367 |
| | RAGE/Vitronectin Ratio | -0.166 | 0.001 | 0.006 | -0.254 | -0.077 | 0.449 |
| | FASLG/EGF Ratio | -0.090 | 0.007 | 0.025 | -0.152 | -0.027 | 0.323 |
| | RAGE/EGF Ratio | -0.135 | 0.001 | 0.006 | -0.207 | -0.064 | 0.455 |
| NP | ApoAII/AXL Ratio | -0.262 | 0.017 | 0.042 | -0.472 | -0.052 | 0.233 |
| | ApoCI/AXL Ratio | -0.332 | 0.0003 | 0.003 | -0.493 | -0.171 | 0.453 |
| | ApoCIII/AXL Ratio | -1023.0 | 0.009 | 0.042 | -1765.0 | -280.943 | 0.271 |
| | ApoE/AXL Ratio | -0.253 | 0.019 | 0.042 | -0.460 | -0.046 | 0.226 |
| | ComFH/AXL Ratio | -0.189 | 0.021 | 0.042 | -0.346 | -0.031 | 0.219 |

Abbreviations: Ang2, Angiopoietin-2; FASLG, Fas ligand receptor; RAGE, Receptor for advanced glycosylation end-products; EGF, Epidermal Growth Factor; Apo, Apolipoprotein; ComFH, Complement Factor H; FDR, false discovery rate.

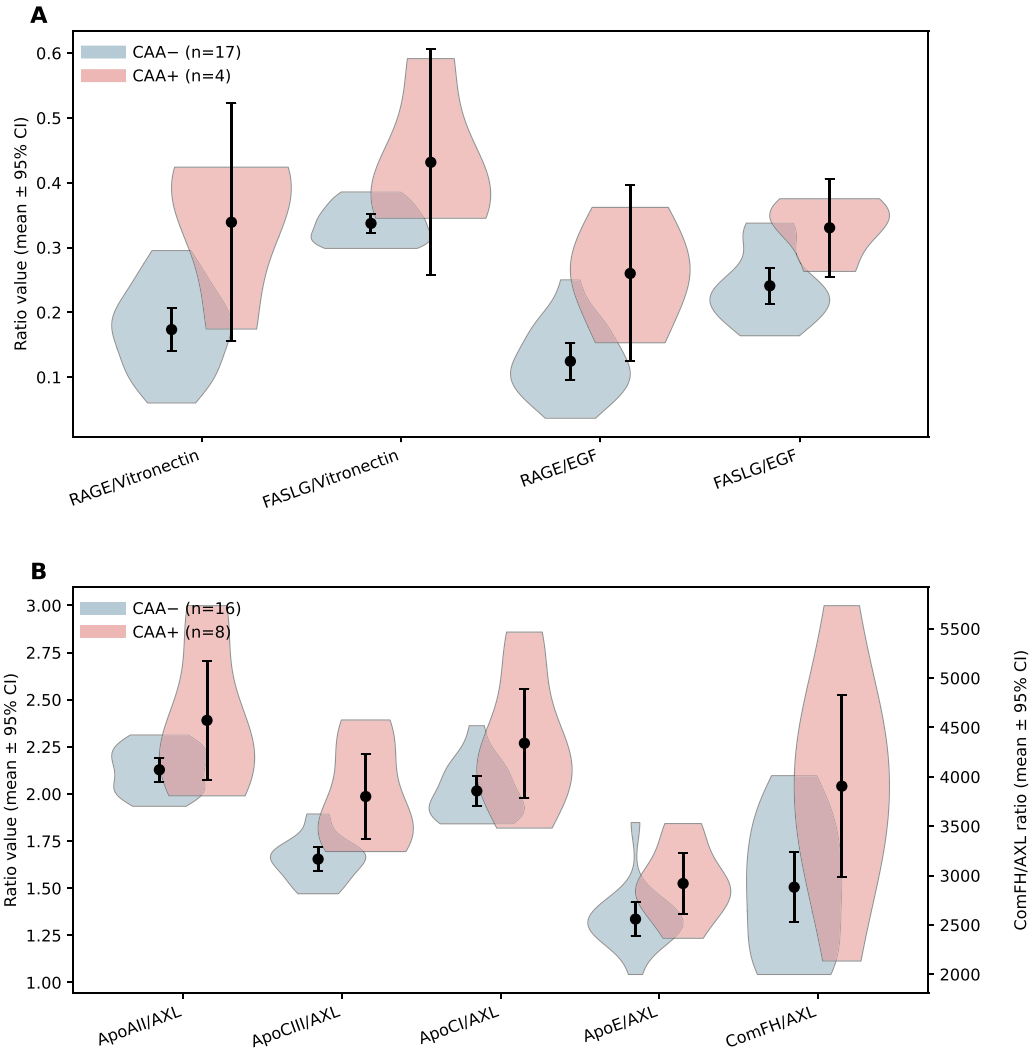


**Fig. 2.** Group means of plasma analytes that significantly differed by CAA status at baseline (T0) in the MRI (A) and neuropathology (B) cohorts. Violins depict the distribution of observed values, while points and error bars indicate mean ± 95% confidence interval. In Panel B, a dual-axis plot with an additional y-axis on the right has been used for visual purposes. *Abbreviations: MRI, magnetic resonance imaging; NP, neuropathology; CAA, cerebral amyloid angiopathy; FASLG, Fas ligand receptor; Receptor for advanced glycosylation end-products; EGF, Epidermal Growth Factor; Apo, Apolipoprotein; ComFH, Complement Factor H; AXL, AXL receptor tyrosine kinase.*

neurodegenerative diseases may include neuroinflammatory or compensatory responses (Chai et al., 2021). However, in sensitivity analyses using dichotomized CAA status, osteopontin-based ratios were not significantly associated, indicating limited robustness of these findings.

Several glycoproteins implicated in amyloid biology—including clusterin and ApoE—were associated with neuropathological CAA severity. Prior studies have demonstrated their upregulation in CAA-affected vessels and suggested context-dependent roles in modulating Aβ aggregation in AD (Foster et al., 2019) and CAA (Endo et al., 2019; Leitner et al., 2024). The apparent elevation of these markers in our cohort may reflect a response to vascular amyloid deposition, although

this interpretation should be considered with caution, given the temporal gap between plasma sampling and neuropathological assessment.

Microglial activity is involved in the pathophysiological pathways leading to CAA pathology, and TAM receptors mediate the glial response to cerebral and vascular Aβ plaques (Hampel et al., 2023; Huang et al., 2021). The stronger associations observed for ratios involving AXL, compared to single analytes such as proinflammatory ApoCIII, may reflect alterations in microglial response dynamics in the context of systemic inflammatory signaling (Zewinger et al., 2020), although this interpretation remains speculative.

Confirmatory studies are required to address potential confounding factors and temporal relationships. While no major differences were observed within cohorts, the overall composition of the cohorts differed, particularly with respect to cognitive status. Furthermore, we restricted the CAA definition to lobar microbleeds as hemorrhagic markers, rather than applying the full Boston criteria v2.0, which allows for defining probable CAA with only one MB when typical non-hemorrhagic findings are present. This approach was chosen to ensure a more consistent definition of probable CAA, given the limited sample size. Consequently, the markers associated with MBs may not be specific to CAA.

Several limitations must be considered. Small sample sizes—particularly in the CAA+ subgroup of the MRI cohort—substantially limit statistical power and increase the risk of both type I and type II errors. Although bootstrap resampling was applied to enhance robustness, such approaches remain vulnerable to sampling variability. In addition, plasma measurements were obtained several years before MRI or neuropathological assessment, introducing temporal heterogeneity that may attenuate associations and limit the biological interpretability of findings, as biomarker levels may not reflect the pathological state at the time of outcome assessment, particularly in the context of disease progression over this interval. Finally, differences in cognitive status between cohorts constrain direct comparisons. These factors underscore the exploratory nature of the findings and the need for replication in larger, well-characterized cohorts.

Ultimately, for participants with concomitant AD pathology, the candidate biomarkers may help to estimate the likelihood of treatment response and risk associated with future combination strategies involving new pharmacological approaches (Cummings et al., n.d.), particularly anti-amyloid antibodies and amyloid-related imaging abnormalities (Hampel et al., 2023).

## CRediT authorship contribution statement

**Orkan Arslan:** Writing – review & editing. **Julian Hellmann-Regen:** Writing – review & editing, Supervision, Conceptualization. **Louise Droste:** Writing – review & editing. **Daria Gref:** Writing – review & editing. **Ersin Ersözlü:** Writing – review & editing, Writing – original draft, Visualization, Formal analysis, Data curation, Conceptualization. **Lukas Preis:** Writing – review & editing. **François Meyer:** Writing – review & editing.

## Acknowledgements

Data collection and sharing for the Alzheimer's Disease Neuroimaging Initiative (ADNI) is funded by the National Institute on Aging (National Institutes of Health Grant U19AG024904). The grantee organization is the Northern California Institute for Research and Education. In the past, ADNI has also received funding from the National Institute of Biomedical Imaging and Bioengineering, the Canadian Institutes of Health Research, and private sector contributions through the Foundation for the National Institutes of Health (FNIH) including generous contributions from the following: AbbVie, Alzheimer's Association; Alzheimer's Drug Discovery Foundation; Araclon Biotech; BioClinica, Inc.; Biogen; BristolMyers Squibb Company; CereSpir, Inc.; Cogstate; Eisai Inc.; Elan Pharmaceuticals, Inc.; Eli Lilly and Company; EuroImmun; F. Hoffmann-La Roche Ltd and its affiliated company Genentech, Inc.; Fujirebio; GE Healthcare; IXICO Ltd.; Janssen Alzheimer Immunotherapy Research & Development, LLC.; Johnson & Johnson Pharmaceutical Research & Development LLC.; Lumosity; Lundbeck; Merck & Co., Inc.; Meso Scale Diagnostics, LLC.; NeuroRx Research; Neurotrack Technologies; Novartis Pharmaceuticals Corporation; Pfizer Inc.; Piramal Imaging; Servier; Takeda Pharmaceutical Company; and Transition Therapeutics.

## Appendix A. Supporting information

Supplementary data associated with this article can be found in the online version at doi:10.1016/j.neurobiolaging.2026.04.004.

## References

Attems, J., Jellinger, K.A., Lintner, F., 2005. Alzheimer's disease pathology influences severity and topographical distribution of cerebral amyloid angiopathy. Acta Neuropathol. 110, 222–231. https://doi.org/10.1007/s00401-005-1064-y.

Bechmann, I., Lossau, S., Steiner, B., Mor, G., Gimsa, U., Nitsch, R., 2000. Reactive astrocytes upregulate Fas (CD95) and Fas ligand (CD95L) expression but do not undergo programmed cell death during the course of anterograde degeneration. Glia 32, 25–41. https://doi.org/10.1002/1098-1136(200010)32:1%253C25::aid-glia30%253E3.0.co;2-y.

Chai, Y.L., Chong, J.R., Raquib, A.R., Xu, X., Hilal, S., Venketasubramanian, N., Tan, B. Y., Kumar, A.P., Sethi, G., Chen, C.P., Lai, M.K.P., 2021. Plasma osteopontin as a biomarker of Alzheimer's disease and vascular cognitive impairment. Sci. Rep. 11, 4010. https://doi.org/10.1038/s41598-021-83601-6.

Charidimou, A., Boulouis, G., Frosch, M.P., Baron, J.-C., Pasi, M., Albucher, J.F., Banerjee, G., Barbato, C., Bonneville, F., Brandner, S., Calviere, L., Caparros, F., Casolla, B., Cordonnier, C., Delisle, M.-B., Deramecourt, V., Dichgans, M., Gokcal, E., Herms, J., Hernandez-Guillamon, M., Jäger, H.R., Jaunmuktane, Z., Linn, J., Martinez-Ramirez, S., Martínez-Sáez, E., Mawrin, C., Montaner, J., Moulin, S., Olivot, J.-M., Piazza, F., Puy, L., Raposo, N., Rodrigues, M.A., Roeber, S., Romero, J. R., Samarasekera, N., Schneider, J.A., Schreiber, S., Schreiber, F., Schwall, C., Smith, C., Szalardy, L., Varlet, P., Viguier, A., Wardlaw, J.M., Warren, A., Wollenweber, F.A., Zedde, M., van Buchem, M.A., Gurol, M.E., Viswanathan, A., Al-Shahi Salman, R., Smith, E.E., Werring, D.J., Greenberg, S.M., 2022. The Boston criteria version 2.0 for cerebral amyloid angiopathy: a multicentre, retrospective, MRI-neuropathology diagnostic accuracy study. Lancet Neurol. 21, 714–725. https://doi.org/10.1016/S1474-4422(22)00208-3.

Choi, C., Benveniste, E.N., 2004. Fas ligand/Fas system in the brain: regulator of immune and apoptotic responses. Brain Res. Brain Res. Rev. 44, 65–81.

Cozza, M., Amadori, L., Boccardi, V., 2023. Exploring cerebral amyloid angiopathy: insights into pathogenesis, diagnosis, and treatment. J. Neurol. Sci. 454, 120866. https://doi.org/10.1016/j.jns.2023.120866.

Cummings, J., Gold, M., Mintun, M., Irizarry, M., von Eschenbach, A., Hendrix, S., Berry, D., Sampaio, C., Sink, K., Landen, J., Kivipelto, M., Grundman, M., Arnold, S.E., Green, A., Partrick, K., Nisenbaum, L., Burstein, A., Fillit, H., n.d. Key Considerations for Combination Therapy in Alzheimer's Clinical Trials: Perspectives from an Expert Advisory Board Convened by the Alzheimer's Drug Discovery Foundation. ⟨https://doi.org/10.1016/j.tjpad.2024.100001⟩.

Endo, Y., Hasegawa, K., Nomura, R., Arishima, H., Kikuta, K.-I., Yamashita, T., Inoue, Y., Ueda, M., Ando, Y., Wilson, M.R., Hamano, T., Nakamoto, Y., Naiki, H., 2019. Apolipoprotein E and clusterin inhibit the early phase of amyloid-β aggregation in an in vitro model of cerebral amyloid angiopathy. Acta Neuropathol. Commun. 7, 12. https://doi.org/10.1186/s40478-019-0662-1.

Foster, E.M., Dangla-Valls, A., Lovestone, S., Ribe, E.M., Buckley, N.J., 2019. Clusterin in Alzheimer's disease: mechanisms, genetics, and lessons from other pathologies. Front. Neurosci. 13, 164. https://doi.org/10.3389/fnins.2019.00164.

Graff-Radford, J., Yong, K.X.X., Apostolova, L.G., Bouwman, F.H., Carrillo, M., Dickerson, B.C., Rabinovici, G.D., Schott, J.M., Jones, D.T., Murray, M.E., 2021. New insights into atypical Alzheimer's disease in the era of biomarkers. Lancet Neurol. 20, 222–234. https://doi.org/10.1016/S1474-4422(20)30440-3.

Grand Moursel, L., van der Graaf, L.M., Bulk, M., van Roon-Mom, W.M.C., van der Weerd, L., 2019. Osteopontin and phospho-SMAD2/3 are associated with calcification of vessels in D-CAA, an hereditary cerebral amyloid angiopathy. Brain Pathol. 29, 793–802. https://doi.org/10.1111/bpa.12721.

Hampel, H., Elhage, A., Cho, M., Apostolova, L.G., Nicoll, J.A.R., Atri, A., 2023. Amyloid-related imaging abnormalities (ARIA): radiological, biological and clinical characteristics. Brain 146, 4414–4424. https://doi.org/10.1093/brain/awad188.

Huang, Y., Happonen, K.E., Burrola, P.G., O'Connor, C., Hah, N., Huang, L., Nimmerjahn, A., Lemke, G., 2021. Microglia use TAM receptors to detect and engulf amyloid β plaques. Nat. Immunol. 22, 586–594. https://doi.org/10.1038/s41590-021-00913-5.

Hyman, B.T., Phelps, C.H., Beach, T.G., Bigio, E.H., Cairns, N.J., Carrillo, M.C., Dickson, D.W., Duyckaerts, C., Frosch, M.P., Masliah, E., Mirra, S.S., Nelson, P.T., Schneider, J.A., Thal, D.R., Thies, B., Trojanowski, J.Q., Vinters, H.V., Montine, T.J., 2012. National Institute on Aging-Alzheimer's Association guidelines for the neuropathologic assessment of Alzheimer's disease. Alzheimers Dement 8, 1–13. https://doi.org/10.1016/j.jalz.2011.10.007.

Jäkel, L., De Kort, A.M., Klijn, C.J.M., Schreuder, F.H.B.M., Verbeek, M.M., 2022. Prevalence of cerebral amyloid angiopathy: a systematic review and meta-analysis. Alzheimers Dement 18, 10–28. https://doi.org/10.1002/alz.12366.

Knudsen, K.A., Rosand, J., Karluk, D., Greenberg, S.M., 2001. Clinical diagnosis of cerebral amyloid angiopathy: validation of the Boston criteria. Neurology 56, 537–539. https://doi.org/10.1212/wnl.56.4.537.

Leitner, D., Kavanagh, T., Kanshin, E., Balcomb, K., Pires, G., Thierry, M., Suazo, J.I., Schneider, J., Ueberheide, B., Drummond, E., Wisniewski, T., 2024. Differences in the cerebral amyloid angiopathy proteome in Alzheimer's disease and mild cognitive impairment. Acta Neuropathol. 148, 9. https://doi.org/10.1007/s00401-024-02767-1.

Love, S., Chalmers, K., Ince, P., Esiri, M., Attems, J., Jellinger, K., Yamada, M., McCarron, M., Minett, T., Matthews, F., Greenberg, S., Mann, D., Kehoe, P.G., 2014. Development, appraisal, validation and implementation of a consensus protocol for the assessment of cerebral amyloid angiopathy in post-mortem brain tissue. Am. J. Neurodegener. Dis. 3, 19–32.

Shaw, L.M., Vanderstichele, H., Knapik-Czajka, M., Clark, C.M., Aisen, P.S., Petersen, R. C., Blennow, K., Soares, H., Simon, A., Lewczuk, P., Dean, R., Siemers, E., Potter, W., Lee, V.M.-Y., Trojanowski, J.Q., Alzheimer's Disease Neuroimaging Initiative, 2009. Cerebrospinal fluid biomarker signature in Alzheimer's disease neuroimaging initiative subjects. Ann. Neurol. 65, 403–413. https://doi.org/10.1002/ana.21610.

Su, J.H., Anderson, A.J., Cribbs, D.H., Tu, C., Tong, L., Kesslack, P., Cotman, C.W., 2003. Fas and Fas Ligand are associated with neuritic degeneration in the AD brain and participate in β-amyloid-induced neuronal death. Neurobiol. Dis. 12, 182–193. https://doi.org/10.1016/s0969-9961(02)00019-0.

Switzer, A.R., Charidimou, A., McCarter, S., Vemuri, P., Nguyen, A.T., Przybelski, S.A., Lesnick, T.G., Rabinstein, A.A., Brown, R.D., Knopman, D.S., Petersen, R.C., Jack, C. R., Jr, Reichard, R.R., Graff-Radford, J., 2024. Boston criteria v2.0 for cerebral amyloid angiopathy without hemorrhage: An MRI-neuropathologic validation study. Neurology 102, e209386. https://doi.org/10.1212/WNL.0000000000209386.

Theodorou, A., Tsantzali, I., Kapaki, E., Constantinides, V.C., Voumvourakis, K., Tsivgoulis, G., Paraskevas, G.P., 2021. Cerebrospinal fluid biomarkers and apolipoprotein E genotype in cerebral amyloid angiopathy. A narrative review. Cereb. Circ. Cogn. Behav. 2, 100010. https://doi.org/10.1016/j.cccb.2021.100010.

Vidoni, E.D., Yeh, H.-W., Morris, J.K., Newell, K.L., Alqahtani, A., Burns, N.C., Burns, J. M., Billinger, S.A., 2016. Cerebral β-amyloid angiopathy is associated with earlier dementia onset in Alzheimer's disease. Neurodegener. Dis. 16, 218–224. https://doi.org/10.1159/000441919.

Weller, R.O., Subash, M., Preston, S.D., Mazanti, I., Carare, R.O., 2008. Perivascular drainage of amyloid-beta peptides from the brain and its failure in cerebral amyloid angiopathy and Alzheimer's disease. Brain Pathol. 18, 253–266. https://doi.org/10.1111/j.1750-3639.2008.00133.x.

Zewinger, S., Reiser, J., Jankowski, V., Alansary, D., Hahm, E., Triem, S., Klug, M., Schunk, S.J., Schmit, D., Kramann, R., Körbel, C., Ampofo, E., Laschke, M.W., Selejan, S.-R., Paschen, A., Herter, T., Schuster, S., Silbernagel, G., Sester, M., Sester, U., Aßmann, G., Bals, R., Kostner, G., Jahnen-Dechent, W., Menger, M.D., Rohrer, L., März, W., Böhm, M., Jankowski, J., Kopf, M., Latz, E., Niemeyer, B.A., Fliser, D., Laufs, U., Speer, T., 2020. Apolipoprotein C3 induces inflammation and organ damage by alternative inflammasome activation. Nat. Immunol. 21, 30–41. https://doi.org/10.1038/s41590-019-0548-1.